ISTITUTO NAZIONALE DI FISICA NUCLEARE

Sezione di Trieste

E. Milotti

LINEAR PROCESSES THAT PRODUCE 1/f OR FLICKER NOISE

Linear processes that produce $1/f$ or flicker noise

Edoardo Milotti

Dipartimento di Fisica dell'Università di Trieste

and

INFN Sezione di Trieste

Via Valerio 2, I-34127 Trieste, Italy

Abstract

$1/f$ noise and flicker noises – i.e. the class of $1/f^\alpha$ noises with $0.5 < \alpha <$ 1.5 – are as ubiquitous as they are mysterious. Several physical mechanisms to generate $1/f$ noise have been devised, and most of them try to obtain a broad, nearly flat distribution of relaxation times, which would then yield a $1/f$ spectrum. However they are all very specialized, and none of them addresses the question of the apparent universality of this noise, while they all fail in some respect. I show here that the power spectral density of a relaxing linear system driven by white noise is determined by the eigenvalue density of the linear operator associated to the system. I also show that the eigenvalue densities of linear operators that reasonably describe diffusion and transport lead to $1/f$ or flicker noise. Using the concepts developed in the paper and a rough approximation of transport in a resistor I derive the Hooge formula for the spectrum of conductance fluctuations.

02.50.Ey, 05.40.+j, 05.60.+w

I. INTRODUCTION

$1/f$ noise appears again and again in many apparently uncorrelated systems as diverse as MOS devices and ocean currents [1–4]. Indeed there are models that justify the occurrence of $1/f$ noise in some systems (see the reviews [5–7]), but they are very specialized, in other words they do not have the "universality" suggested by the ubiquity of $1/f$ noise. It is generally accepted that the mechanism that leads to $1/f$ noise is a system with an exponential response function driven by a shot noise source, and such that the relaxation times of the system are chosen at random from a very broad, flat distribution. The power spectral density (PSD) of a simple relaxation process with characteristic time τ and rate $\lambda = 1/\tau$ is proportional to $1/(\omega^2 + \lambda^2)$ (ω is the angular frequency), and if the rates are uniformly distributed between the limits λ_{min} and λ_{max}, then the PSD is given by the integral

$$S(\omega) \propto \int_{\lambda_{min}}^{\lambda_{max}} \frac{d\lambda}{\omega^2 + \lambda^2} = \frac{1}{\omega} \left(\arctan \frac{\lambda_{max}}{\omega} - \arctan \frac{\lambda_{min}}{\omega} \right). \tag{1}$$

Then if $\lambda_{min} \ll \omega \ll \lambda_{max}$, $S(\omega) \propto 1/\omega$, and thus a flat distribution yields a $1/f$ spectrum. Furthermore such a distribution gives a stationary Gaussian process if the driving noise source is itself stationary and Gaussian, and this agrees well with most experimental observations of the statistical properties of $1/f$ noise, and also seems to rule out all explanations that relate this noise to some underlying nonlinear dynamics. However, as Press puts it in his nice review paper [1], "it [is] hard to conceive ... physical mechanisms which contribute stretched pulses with just the right frequency of occurrence over, say, six orders of magnitude. Scale superposition just transfers the mystery to the random 'stretching factor' process."

I suggest here a fairly general explanation which depends only on very weak assumptions: the PSD of a linear system [8] driven by white Gaussian noise is uniquely determined by the eigenvalue density of the associated linear operator, and the (linear) operators that describe several systems that exhibit flicker noise, and in particular diffusion and transport, have densities that lead to $1/f$ or flicker noise – i.e. to $1/f^\alpha$ noises with $0.5 < \alpha < 1.5$.

2

This is a purely mathematical device that does not depend on the underlying physics, and there is no need to introduce a "stretching factor". Although the mathematics developed here is applicable to many systems that are totally unrelated to $1/f$ current noise, the main application of a flicker noise theory is the "explanation" of $1/f$ current noise. This requires a description of charge transport and diffusion, and here I make an attempt to go in this direction, but I do not develop a complete theory of flicker noise in resistors. It must be remarked that diffusion processes have been repeatedly invoked as the source of $1/f$ noise in resistors, most notably by Voss and Clark [9] who have introduced a diffusion model based on temperature fluctuations. The model described in this paper is based on number fluctuations - and therefore has a much wider applicability - and goes further in the analysis thanks to a considerably simpler mathematical formalism.

Section II outlines the connection between diffusion, transport, and systems of linear differential equations of the relaxation type. The PSD is discussed in section III, while in section IV I return to the description of section II and derive lower and upper bounds for the eigenvalues. Section V exhibits classes of processes that actually convert white noise to $1/f$ or flicker noise. A simple transport channel that may roughly model a resistor is described in section VI, and it is shown that this model leads to the Hooge formula for conductance fluctuations. Notice that no special distinction is made, throughout the paper, between "equilibrium" and "transport" noise.

II. DIFFUSION AND TRANSPORT PROCESSES ON A DISCRETE SET OF SITES

Several measurements [5–7,9] indicate that $1/f$ noise in resistors exists at equilibrium, and therefore that it may be due to some sort of diffusion. Thus we start here with pure diffusion and consider a population of N non-interacting random walkers distributed over n sites, so that $N_k(t)$ is the population of the k-th site at time t, and $a_{kj}dt$ is the probability that a random walker which is at site j jumps to site k during the time interval $(t, t+dt)$. At

3

present no special topology is associated with the n sites, however we make the additional hypothesis $N \gg n$; as we shall see later this is not a serious restriction.

Then the number of random walkers that jump from site j to site k during $(t, t+dt)$ is a random variable with a binomial distribution, with average and variance both equal to $a_{kj}N_j(t)dt$. The total number of random walkers that jump *to* k is then (in the limit of large N_j) a Gaussian variate with average and variance both equal to

$$\sum_{\substack{j=1,n \\ j \neq k}} a_{kj}N_j(t)dt. \tag{2}$$

The total number of random walkers that jump *away* from site k during the same time interval is still another Gaussian variate with average and variance both equal to

$$\sum_{\substack{j=1,n \\ j \neq k}} a_{jk}N_k(t)dt = N_k(t) \sum_{\substack{j=1,n \\ j \neq k}} a_{jk}dt = \frac{1}{\tau_k}N_k(t)dt. \tag{3}$$

Therefore the net change of the population $N_k(t)$ during the time interval $(t, t+dt)$ is

$$dN_k = -\frac{1}{\tau_k}N_k(t)dt + \sum_{\substack{j=1,n \\ j \neq k}} a_{kj}N_j(t)dt + \nu_k(t)dt, \tag{4}$$

where $\nu_k(t)$ is to a good approximation a Gaussian noise process with

$$\langle \nu_k(t) \rangle = 0, \tag{5a}$$

$$\langle \nu_j(t)\nu_k(t') \rangle = \sigma_k^2 \delta_{jk}\delta(t-t'), \tag{5b}$$

$$\sigma_k^2 = \sum_{\substack{j=1,n \\ j \neq k}} a_{kj}N_j(t) + \sum_{\substack{j=1,n \\ j \neq k}} a_{jk}N_k(t) \approx \sum_{\substack{j=1,n \\ j \neq k}} (a_{kj}\langle N_j \rangle + a_{jk}\langle N_k \rangle) \tag{5c}$$

(here $\langle \ldots \rangle$ denotes the ensemble average). Until now nothing has been said about the nature of the random walkers: usually they are assumed to be conserved in number, but this is not the case here. In writing equations (4) and (5) we have introduced the hypothesis that they are conserved only on average, so that the fluctuations about the average population changes are uncorrelated. While this may seem strange at first, as it is a rather uncommon

4

deviation from the usual random-walk formalism, it is indeed a much more natural assumption, since such processes as charge carrier pair creation and recombination (in conductors), or pressure fluctuations due to fluid compressibility (in fluid flow), destroy the correlations. This also means that equation (5c) underestimates the white noise variance. However, as we shall see later, this affects only the total noise power and not the shape of the PSD. Introducing the vectors $\boldsymbol{N} = \{N_k\}_{k=1,\ldots,n}$, $\boldsymbol{\nu} = \{\nu_k\}_{k=1,\ldots,n}$ and the matrix $A = \{a_{jk}\}_{j,k=1,\ldots,n}$ with $a_{kk} = -\frac{1}{\tau_k}$, we can rewrite equation (4) in vector form:

$$dN = AN dt + \boldsymbol{\nu} dt. \tag{6}$$

Now assume that the sites $1,\ldots,n$ are chained together so that site k is adjacent to sites $k-1$ and $k+1$. Then ordinary diffusion due to the simple 1D unbiased random walk can be recovered if we let $n \to \infty$, $a_{jj} = -\frac{1}{\tau}$, $a_{k,k\pm1} = \frac{1}{2\tau}$, and $a_{jk} = 0$ if $j \neq k, k\pm1$. In fact from definition (3), τ_k is given by $\tau_k = (a_{k-1,k} + a_{k+1,k})^{-1}$ and therefore $\tau_k = \tau$ is the same for all k's, and

$$dN_k = -\frac{1}{\tau}N_k(t)dt + \frac{1}{2\tau}(N_{k+1}(t) + N_{k-1}(t))dt + \nu_k(t)dt. \tag{7}$$

Then taking the ensemble average, introducing the position variable $x = k\Delta x$, and denoting $N(x,t) = \langle N_k(t) \rangle$, where Δx is the (small) distance between adjacent sites, we find

$$dN(x,t) = -\frac{1}{\tau}N(x,t)dt + \frac{1}{2\tau}(N(x+\Delta x, t) + N(x-\Delta x, t))dt. \tag{8}$$

Eventually, if Δx is very small we can write

$$\frac{\partial N}{\partial t} = \frac{1}{2}D\frac{\partial^2 N}{\partial t^2}, \tag{9}$$

where $D = \Delta x^2/\tau$ is the diffusion constant, and this is just the usual forward Fokker-Planck equation (for the average values $N(x,t)$) for the simple random walk (see, e.g., [10]). Similarly if we take the same topology and let $a_{jj} = -\frac{1}{\tau}$, $a_{j,j-1} = \frac{p}{\tau}$, $a_{j,j+1} = \frac{q}{\tau}$ with $p+q = 1$, $p, q \geq 0$, and $a_{jk} = 0$ if $j \neq k\pm1$, we obtain the forward Fokker-Planck equation for diffusion + transport (for the biased 1D simple random walk, see reference [10])

5

$$\frac{\partial N}{\partial t} = \frac{1}{2}D\frac{\partial^2 N}{\partial t^2} - v\frac{\partial N}{\partial x} \tag{10}$$

with drift speed $v = (p - q)\Delta x/\tau$ and the same diffusion constant D as before.

III. POWER SPECTRAL DENSITIES

We introduce now the spectral representations for the populations and for the noise processes:

$$N_k(t) = \frac{1}{2\pi}\int_{-\infty}^{+\infty} e^{i\omega t}F_k(\omega)d\omega, \tag{11}$$

$$\nu_k(t) = \frac{1}{2\pi}\int_{-\infty}^{+\infty} e^{i\omega t}f_k(\omega)d\omega. \tag{12}$$

Then, proceeding as in [11] and using equation (6), we can write:

$$i\omega F(\omega) = AF(\omega) + f(\omega), \tag{13}$$

where $F(\omega) = \{F_k(\omega)\}_{k=1,...,n}$ and $f(\omega) = \{f_k(\omega)\}_{k=1,...,n}$ are the vectors of Fourier transforms. The last equation can be solved formally for $F(\omega)$, and we find

$$F(\omega) = (i\omega\mathbb{1} - A)^{-1}f(\omega), \tag{14}$$

($\mathbb{1}$ is the identity matrix) so that, using the definition given in [12], the PSD of the stochastic process $N_k(t)$ is

$$S_k(\omega) = \lim_{T\to\infty}\frac{\langle|F_k(\omega)|^2\rangle}{2\pi T} = \lim_{T\to\infty}\frac{\langle|\sum_{j=1}^{n}(i\omega\mathbb{1} - A)_{kj}^{-1}f_j(\omega)|^2\rangle}{2\pi T} \tag{15}$$

(in this formula the process $N_k(t)$ is assumed to be nonzero in a time interval of duration T). From the independence of the stochastic processes $\{\nu_k\}$ it follows that

$$S_k(\omega) = \sum_{j=1}^{n}|(i\omega\mathbb{1} - A)_{kj}^{-1}|^2 \lim_{T\to\infty}\frac{\langle|f_j(\omega)|^2\rangle}{2\pi T} \tag{16}$$

$$= \sum_{j=1}^{n}|(i\omega\mathbb{1} - A)_{kj}^{-1}|^2 s_j(\omega) \tag{17}$$

6

where $s_j(\omega)$ is the power spectral density of ν_j, i.e. $s_j(\omega) = \sigma_j^2/2\pi$.

Formally this solves the problem of finding the PSD. To proceed further me must make assumptions on the PSD's of the individual noise processes that drive the system. Since we are mostly concerned with noise in uniform systems, we assume that all the PSD's are the same, i.e. $\sigma_j^2 = \sigma^2$ for all j. We also assume that $a_{jk} = a_{kj}$ (i.e. the interaction between different sites is symmetric) and that the eigenvalues of A are not degenerate. Then the eigenvalues $\{\lambda_k\}_{k=1,\ldots,n}$ of A are real and there is an orthonormal basis of real eigenvectors $\{\boldsymbol{\eta}_k\}_{k=1,\ldots,n}$ such that $A\boldsymbol{\eta}_k = \lambda_k\boldsymbol{\eta}_k$. Using this basis we can write

$$\boldsymbol{F}(\omega) = \sum_{k=1}^{n} \Gamma_k(\omega)\boldsymbol{\eta}_k, \tag{18}$$

$$\boldsymbol{f}(\omega) = \sum_{k=1}^{n} \gamma_k(\omega)\boldsymbol{\eta}_k, \tag{19}$$

and substituting in equation (13) we obtain

$$\sum_{k=1}^{n}(i\omega - \lambda_k)\Gamma_k(\omega)\boldsymbol{\eta}_k = \sum_{k=1}^{n} \gamma_k(\omega)\boldsymbol{\eta}_k. \tag{20}$$

Because of the orthogonality of $\{\boldsymbol{\eta}_k\}$, equality holds for each component, i.e.

$$\Gamma_k(\omega) = \frac{\gamma_k(\omega)}{(i\omega - \lambda_k)}, \tag{21}$$

and therefore

$$F_k(\omega) = \sum_{j=1}^{n} \frac{\gamma_j(\omega)}{(i\omega - \lambda_j)}(\boldsymbol{\eta}_j)_k. \tag{22}$$

The PSD is proportional to

$$\langle |F_k(\omega)|^2 \rangle = \langle |\sum_{j=1}^{n} \frac{\gamma_j(\omega)}{(i\omega - \lambda_j)}(\boldsymbol{\eta}_j)_k|^2 \rangle$$
$$= \sum_{j=1}^{n} \frac{\langle |\gamma_j|^2 \rangle}{\omega^2 + \lambda_j^2}|(\boldsymbol{\eta}_j)_k|^2 + \sum_{\substack{j,l \\ j \neq l}} \frac{\langle \gamma_j\gamma_l^* \rangle}{(i\omega + \lambda_j)(-i\omega + \lambda_l)}(\boldsymbol{\eta}_j)_k(\boldsymbol{\eta}_l^*)_k, \tag{23}$$

and similarly

7

$$\langle |f_k(\omega)|^2 \rangle = \langle | \sum_{j=1}^{n} \gamma_j(\omega)(\boldsymbol{\eta}_j)_k |^2 \rangle$$

$$= \sum_{j=1}^{n} \langle |\gamma_j|^2 \rangle |(\boldsymbol{\eta}_j)_k|^2 + \sum_{\substack{j,l \\ j \neq l}} \langle \gamma_j \gamma_l^* \rangle (\boldsymbol{\eta}_j)_k (\boldsymbol{\eta}_l^*)_k. \tag{24}$$

We have already assumed that at each site a random walker sees the same average environment i.e. $\sigma_k = \sigma$ for all k's. Then both the vector $\boldsymbol{\nu}$ and the vectors of Fourier transforms $\boldsymbol{f}(\omega)$ are distributed with spherical symmetry in their n-dimensional spaces, and a rotation does not change the symmetry properties of the distributions. Therefore using $\{\boldsymbol{\eta}_k\}$ as a basis the stochastic processes $\{\gamma_k\}$ are still independent in the sense that $\langle \gamma_j(\omega) \gamma_k^*(\omega') \rangle = 0$ if $j \neq k$ and $\omega \neq \omega'$, and $\langle |\gamma_j(\omega)|^2 \rangle = \langle |f_k(\omega)|^2 \rangle$ for all j, k. Now we make use of the normalization conditions for the vectors $\boldsymbol{\eta}_k$, i.e. $\sum_{j=1}^{n} |(\boldsymbol{\eta}_k)_j|^2 = 1$, and assume a uniform distribution of the eigenvector directions so that $\int_{\lambda_0}^{\lambda_0 + \Delta\lambda} |[\boldsymbol{\eta}(\lambda)]_k|^2 d\lambda \approx \Delta\lambda/n$. Then equation (23) becomes:

$$\langle |F(\omega)|^2 \rangle = \langle |F_k(\omega)|^2 \rangle = \sum_{j=1}^{n} \frac{\langle |\gamma_j|^2 \rangle}{\omega^2 + \lambda_j^2} |(\boldsymbol{\eta}_j)_k|^2 \approx \langle |\gamma(\omega)|^2 \rangle \int_{\lambda_{min}}^{\lambda_{max}} \frac{f_A(\lambda)}{\omega^2 + \lambda^2} d\lambda, \tag{25}$$

where we have dropped the index k, since now all the spectral densities are the same, and where λ_{min} and λ_{max} are the minimum and maximum eigenvalues, and $f_A(\lambda)$ is the eigenvalue density of the matrix A, normalized so that $\int_{\lambda_{min}}^{\lambda_{max}} f_A(\lambda) d\lambda = 1$. Moreover $s_j(\omega) = \sigma^2/2\pi$ and we get eventually:

$$S(\omega) = \frac{\sigma^2}{2\pi n} \sum_{j=1}^{n} \frac{1}{\omega^2 + \lambda_j^2} \tag{26}$$

$$\approx \frac{\sigma^2}{2\pi} \int_{\lambda_{min}}^{\lambda_{max}} \frac{f_A(\lambda)}{\omega^2 + \lambda^2} d\lambda. \tag{27}$$

Thus the shape of the spectrum $S(\omega)$ is determined by the eigenvalue density $f_A(\lambda)$ of the matrix A, and if it is nearly constant in the interval (λ_a, λ_b) (with $\lambda_a \ll \lambda_b$), then $S(\omega)$ has a $1/f$ dependence in the region $\lambda_a \ll \omega \ll \lambda_b$. (A different derivation and an extension of these results to the case of transport is given in Appendix A).

IV. LOWER AND UPPER BOUNDS

We use now the Perron and the Gershgorin theorems to derive lower and upper bounds for the eigenvalues of the relaxation matrices introduced in section II. These matrices have the general form:

$$A = \begin{pmatrix} -\dfrac{1}{\tau_1} & a_{12} & a_{13} & \cdots \\ a_{21} & -\dfrac{1}{\tau_2} & a_{23} & \cdots \\ a_{31} & a_{32} & -\dfrac{1}{\tau_3} & \cdots \\ \vdots & \vdots & \vdots & \ddots \end{pmatrix}; \tag{28}$$

with negative diagonal elements, while all nondiagonal elements are non-negative. We define first the matrix $A' = A + \frac{1}{\tau_{min}}\mathbb{1}$, where $\tau_{min} = \min_k\{\tau_k\}$, so that A' and A share the same eigenvectors, while the eigenvalues are shifted:

$$A'\boldsymbol{\eta}_k = \left(A + \frac{1}{\tau_{min}}\mathbb{1}\right)\boldsymbol{\eta}_k = \left(\lambda_k + \frac{1}{\tau_{min}}\right)\boldsymbol{\eta}_k = \lambda'_k\boldsymbol{\eta}_k. \tag{29}$$

Now A' is a non-negative matrix and the Perron theorem applies [13], with the result that there is a real eigenvalue λ'_{max} such that for any other eigenvalue α' of A' the inequality $|\alpha'| < \lambda'_{max}$ holds, and λ'_{max} satisfies the following inequality:

$$\lambda'_{max} \leq \max_k\left\{\sum_{j=1}^{n} a'_{jk}\right\} = \max_k\left\{\frac{1}{\tau_{min}} - \frac{1}{\tau_k} + \sum_{\substack{j=1,n \\ j\neq k}} a_{jk}\right\} = \frac{1}{\tau_{min}}. \tag{30}$$

The inequality for the corresponding eigenvalues of A becomes $\lambda_{max} \leq 0$, so that all the eigenvalues of A are non-positive. Now a question arises: when is A singular, i.e. when is 0 its maximum eigenvalue? This is very important for the PSD, since the sum (26) diverges quadratically when $\omega \to 0$ if 0 is an eigenvalue of A. To answer this question we go back to equation (6) and notice that the corresponding equation for the average values is

$$\frac{d\langle \boldsymbol{N}\rangle}{dt} = A\langle \boldsymbol{N}\rangle. \tag{31}$$

It is well known that this system of linear differential equations is asymptotically stable if and only if all the eigenvalues of A are negative [14], and in this case $\langle \boldsymbol{N}\rangle$ approaches the

9

null vector as $t \to \infty$. The conclusion is that 0 is an eigenvalue of A if and only if the average total population $\langle N \rangle = \sum_{k=1}^{n} \langle N_k \rangle$ is conserved. This is indeed the case for the relaxation matrices defined above, since the underlying kinetics conserves the (average) number of random walkers. However it is also clear that such a system cannot be observed, and that whenever an observer perturbs it there must be some loss so that the greatest eigenvalue of A must be at least slightly negative. This may be rephrased saying that the observer must extract a fraction of the population at some site to carry out his observations on the system. This means also that with the inclusion of an observer the multivariate stochastic process is not stationary as long as there are non-zero populations. And even in the case in which there is no observer the process is not stationary in the limit of infinite total population. In fact the sum (26) diverges quadratically as ω approaches 0, and therefore the correlation function also diverges (as it does for the simple random walk). In a short while we shall introduce more realistic stationary models with non-zero equilibrium states.

While it is clear that the most relevant part of the eigenvalue density lies near the origin, since it determines the behavior of the PSD in the low-frequency limit, it is interesting to notice that the same upper bound and also a lower bound can be found assuming that A is symmetric and using the Gershgorin theorem [13]. In this case the Gershgorin theorem states that every eigenvalue λ satisfies at least one of the inequalities:

$$- \sum_{\substack{j=1,n \\ j \neq k}} a_{kj} \leq \lambda - \frac{1}{\tau_k} \leq \sum_{\substack{j=1,n \\ j \neq k}} a_{kj} \tag{32}$$

i.e. all the eigenvalues are contained in the range

$$-\frac{2}{\tau_{min}} \leq \lambda \leq 0. \tag{33}$$

The idealized systems that we have studied so far look promising but have divergent PSD's and cannot be stationary (except in the case of vanishing populations N_k). However in real-life systems there is usually a noisy input and an output, so that equations (4) should be modified accordingly:

10

$$dN_k = -\frac{1}{\tau_k}N_k(t)dt + \sum_{\substack{j=1,n \\ j \neq k}} a_{kj}N_j(t)dt + \nu_{0,k}dt + \nu_k(t)dt, \tag{34}$$

where $\nu_0 = \{\nu_{0,k}\}_{k=1,...,n}$ is a constant vector, which is the average value of the noisy input, and where

$$\frac{1}{\tau_k} \geq \sum_{\substack{j=1,n \\ j \neq k}} a_{jk}. \tag{35}$$

Moreover (35) must be a strict inequality for at least one site, so that there is at least one output site. The requirement of uniform behavior is satisfied by assuming that the transition probabilities to neighboring sites are always the same.

Typically – for a given topology – we can identify an "inside" and a "boundary" for any set of sites. Then the random walkers in the inside can usually jump only to neighboring sites – and the equal sign holds in (35) – while the random walkers on the boundary can jump out of the system and (35) is a strict inequality. We also assume that any site can be reached from any other site with a finite sequence of jumps, and that the reverse path is also physically possible, then the matrix A must be irreducible, and because of (35) it is diagonally dominant, therefore it must be invertible and 0 is not an eigenvalue (see theorem 6.2.27 in [13]). Combining this result with the loose bounds from the Perron and the Gershgorin theorem that we found above, we see that all the eigenvalues are negative and that the deterministic part of the stochastic processes N_k is stable with nonzero N_k's. Moreover the statistical descriptions (5a) and (5b) for the stochastic processes ν still hold.

The vector form of equation (34) is:

$$dN = ANdt + \nu_0dt + \nu dt, \tag{36}$$

while the corresponding equation for the average values is

$$d\langle N \rangle = A\langle N \rangle dt + \nu_0dt, \tag{37}$$

and subtracting equation (37) from (36) we get

$$d\left(N - \langle N \rangle\right) = A\left(N - \langle N \rangle\right) + \nu, \tag{38}$$

11

therefore the spectral results derived in the previous section apply unchanged to the variates $N_k - \langle N_k \rangle$. Notice that equation (37) can easily be solved and it is well-known that the general solution is [14]

$$\langle N_k \rangle = \{Te^{Dt}T^{-1}N_0\}_k + \langle N_k \rangle_{eq} \tag{39}$$

$$= \sum_{j=1}^{n} w_{kj}e^{\lambda_j t} + \langle N_k \rangle_{eq}, \tag{40}$$

where N_0 is the vector of initial values, $\langle N_k \rangle_{eq}$ are the equilibrium values

$$\langle N_k \rangle_{eq} = - \left(A^{-1}\nu_0 \right)_k, \tag{41}$$

$D = diag(\lambda_1, \ldots, \lambda_n)$, and T is a matrix whose columns are the eigenvectors of A.

V. THE EIGENVALUE DENSITIES FOR SOME DIFFUSION AND TRANSPORT OPERATORS

We turn now to a detailed analysis of the eigenvalue densities of some linear operators. We take first the case of diffusion along a linear chain of n sites with hopping to nearest neighbors only (the process described at the end of section II), which is associated to the $n \times n$ matrix:

$$A = \begin{pmatrix} -\frac{1}{\tau} & \frac{1}{2\tau} & 0 & 0 & 0 & \cdots \\ \frac{1}{2\tau} & -\frac{1}{\tau} & \frac{1}{2\tau} & 0 & 0 & \cdots \\ 0 & \frac{1}{2\tau} & -\frac{1}{\tau} & \frac{1}{2\tau} & 0 & \cdots \\ 0 & 0 & \frac{1}{2\tau} & -\frac{1}{\tau} & \frac{1}{2\tau} & \cdots \\ \vdots & \vdots & \vdots & \vdots & \vdots & \ddots \end{pmatrix}. \tag{42}$$

Using elementary methods it is easy to show that the eigenvalues of this (symmetric) matrix are:

$$\lambda_m = -\frac{1}{\tau}\left(1 - \cos\frac{\pi m}{n+1}\right) \qquad (m = 1, \ldots, n) \tag{43}$$

Therefore the corresponding density for $n \gg 1$ is

12

$$f_A(\lambda) \approx \frac{1}{n}\left(\frac{dm}{d\lambda_m}\right) \approx \frac{1}{\pi}\frac{1}{\sqrt{|\lambda|(\frac{2}{\tau} - |\lambda|)}} \qquad \left(-\frac{2}{\tau} + \frac{\pi^2}{2\tau n^2} < \lambda < -\frac{\pi^2}{2\tau n^2}\right), \qquad (44)$$

which is dominated by the two large peaks near 0 and near $-\frac{2}{\tau}$. The PSD can be computed directly from (26) and the result is

$$
\begin{aligned}
S(\omega) &\approx \frac{\sigma^2}{2\pi n}\sum_{m=1}^{n}\frac{1}{\omega^2 + \lambda^2}\\
&\approx \frac{\sigma^2\tau^2}{2\pi}\int_{1/n}^{1-1/n}\frac{dx}{\omega^2\tau^2 + (1 - \cos\pi x)^2}
\end{aligned}
\qquad (45)
$$

From the integral expression (45), it is clear that if $\omega\tau \gg 1$ then $S(\omega) \propto 1/\omega^2$, and if $\omega\tau \ll 1/n^2$ then $S(\omega)$ is approximately constant. In the intermediate region $1 \gg \omega\tau \gg 1/n^2$ the PSD follows approximately the power law $1/f^{1.5}$ as shown in figure 1, where the PSD (45) is plotted for different values of n. The complete integrated form of (45) is quite lengthy, and it is difficult to use it to extract the $1/f^{1.5}$ power law. However a derivation of the $1/f^{1.5}$ power law for $n \gg 1$ is given in appendix B.

Thus simple 1D diffusion yields a flicker noise, and if n is sufficiently large the effect spans many orders of magnitude. Figure 1 shows that for $n = 500$ the $1/f^{1.5}$ region spans almost four decades, and for large n the $1/f^{1.5}$ region spans approximately $\log_{10}\left|\frac{\lambda_{min}}{\lambda_{max}}\right| \approx 2\log_{10} n$ decades. The PSD is well-behaved, and the correlation function computed from the Wiener-Kintchine theorem is free of divergences both at low and at high frequency.

Many features of this 1D diffusion model are shared by all the relaxation operators introduced in section IV. We have shown that all the eigenvalues are contained in a range $\lambda_{min} \leq \lambda \leq \lambda_{max} < 0$, and therefore the PSD always approaches the (finite) value $\frac{1}{n}\sum_{k=1}^{n}\frac{1}{\lambda_k^2}$ as ω approaches 0. At the same time the derivative also approaches 0, therefore every PSD flattens to a constant value near the origin. Moreover the eigenvalue range is bounded, therefore for ω large enough, the PSD has a $1/f^2$ behavior, and there must be an intermediate region that interpolates between these behaviors. We have just seen that it may span several orders of magnitude, and it is on this intermediate region that we shall focus our attention from now on. Another important feature shared by the whole class of relaxation operators is that the processes are linear, while the driving noise sources are stationary and Gaussian, therefore

13

the relaxation processes N_k are also Gaussian. Furthermore the deterministic part of each process has a simple attractor (since the eigenvalues of A are all negative), therefore the process has a finite variance [15], and it is stationary. This agrees well with past experimental observations of the statistical properties of $1/f$ noise (see the references in the reviews [5–7]). As an independent check of the analytical calculations, I have set up a Monte Carlo program to simulate a 1D chain. The populations at each site are updated according to

$$\Delta N_k = \sum_{j=1}^{n} a_{kj} N_j \Delta t + \nu_{0,k} \Delta t + \sigma_k R_k, \tag{46}$$

where the R_k's are Gaussian pseudo-random numbers with zero mean and unit standard deviation, and the actual standard deviation σ_k of each ΔN_k is computed from the formula

$$\sigma_k^2 = \sum_{j=1}^{n} |a_{kj} \langle N_j \rangle \Delta t| + |\nu_{0,k} \Delta t|. \tag{47}$$

The gaussian pseudo-random numbers R_k have been generated with the routine `gasdev` described in [16], and modified to use the uniform pseudo-random number generator `ran2` instead of the faster but less safe `ran1` (they are both in the program library [16]).

The simulation included an external noise source at each end of the chain, and the sites have been initialized with the resulting equilibrium values (which are further discussed in the next section). Figure 2 shows a small part of the simulated signal, while figure 3 shows the PSD of the simulated process, which provides a nice confirmation of the theoretical result.

Now the simple 1D diffusion model can be made more "realistic" either by allowing jumps to more distant sites, or stepping up in the number of dimensions. Let us start with a 1D diffusion process with a probability of jumping from site j to site k that decreases quadratically with the distance $|j - k|$. Now we take matrix elements $a_{jk} = \frac{\kappa}{|j-k|^2}$, $a_{kk} = -\frac{1}{\tau} = -\max_k \left\{ \sum_{j \neq k} a_{jk} \right\}$. The associated relaxation matrix is:

$$A = \begin{pmatrix} -\frac{1}{\tau} & \kappa & \frac{\kappa}{4} & \frac{\kappa}{9} & \frac{\kappa}{16} & \cdots \\ \kappa & -\frac{1}{\tau} & \kappa & \frac{\kappa}{4} & \frac{\kappa}{9} & \cdots \\ \frac{\kappa}{4} & \kappa & -\frac{1}{\tau} & \kappa & \frac{\kappa}{4} & \cdots \\ \frac{\kappa}{9} & \frac{\kappa}{4} & \kappa & -\frac{1}{\tau} & \kappa & \cdots \\ \vdots & \vdots & \vdots & \vdots & \vdots & \ddots \end{pmatrix}, \tag{48}$$

14

with $\frac{1}{\tau} \approx 2\kappa \sum_{n=0}^{\infty} \frac{1}{n^2} = \frac{\kappa\pi^2}{3}$. We can still find the eigenvalues of this matrix by elementary methods, and they are:

$$\tau\lambda_m = -3\left(\frac{m}{n+1} - \frac{m^2}{2(n+1)^2}\right) \qquad (m=1,\ldots,n). \tag{49}$$

This expression is exact for $n \to \infty$, however it gives a fairly good approximation of the eigenvalues of matrices like (48) even when their dimension is not too large: figure 4 shows that the eigenvalue density obtained from the eigenvalues computed with the numerical Jacobi method [16] for $n = 50$, is practically indistinguishable - at the scale of the plot - from the density derived from (49). The eigenvalue density in figure 4 is nearly flat in a large region near the origin, therefore we expect to find a large $1/f$ region in the PSD. Indeed, using (26) and the eigenvalues obtained numerically, we obtain the curve shown in figure 5 for $n = 50$ and $\kappa = 1$, where an extended $1/f$ region is clearly visible. This nice $1/f$ behavior is the exception rather than the rule for one-dimensional systems, which are more prone to follow the behavior displayed by the nearest neighbor interactions described at the beginning of this section (see figures 6 and 7).

We consider now two- and three-dimensional lattices with hopping to nearest neighbors only. Take, e.g., a 3×3, 2D lattice with the sites labeled

$$
\begin{array}{ccc}
1 & 2 & 3 \\
4 & 5 & 6 \\
7 & 8 & 9
\end{array}
$$

so that the associated matrix is:

$$A = \begin{pmatrix}
-\frac{1}{\tau} & \frac{1}{4\tau} & 0 & \frac{1}{4\tau} & 0 & 0 & 0 & 0 & 0 \\
\frac{1}{4\tau} & -\frac{1}{\tau} & \frac{1}{4\tau} & 0 & \frac{1}{4\tau} & 0 & 0 & 0 & 0 \\
0 & \frac{1}{4\tau} & -\frac{1}{\tau} & \frac{1}{4\tau} & 0 & \frac{1}{4\tau} & 0 & 0 & 0 \\
\frac{1}{4\tau} & 0 & \frac{1}{4\tau} & -\frac{1}{\tau} & \frac{1}{4\tau} & 0 & \frac{1}{4\tau} & 0 & 0 \\
0 & \frac{1}{4\tau} & 0 & \frac{1}{4\tau} & -\frac{1}{\tau} & \frac{1}{4\tau} & 0 & \frac{1}{4\tau} & 0 \\
0 & 0 & \frac{1}{4\tau} & 0 & \frac{1}{4\tau} & -\frac{1}{\tau} & \frac{1}{4\tau} & 0 & \frac{1}{4\tau} \\
0 & 0 & 0 & \frac{1}{4\tau} & 0 & \frac{1}{4\tau} & -\frac{1}{\tau} & \frac{1}{4\tau} & 0 \\
0 & 0 & 0 & 0 & \frac{1}{4\tau} & 0 & \frac{1}{4\tau} & -\frac{1}{\tau} & \frac{1}{4\tau} \\
0 & 0 & 0 & 0 & 0 & \frac{1}{4\tau} & 0 & \frac{1}{4\tau} & -\frac{1}{\tau}
\end{pmatrix}, \tag{50}$$

so that the probability of jumping to any given neighboring site is always the same, the relaxation time is also the same for all sites, and the random walkers can leave the lattice from all the $(2n_x + 2n_y - 4)$ sites on the boundary. Once again it is easy to show that for a rectangular lattice of $n_x \times n_y$ sites the eigenvalues are:

$$\lambda_{jk} = -\frac{1}{2\tau}\left(2 - \cos\frac{\pi j}{n_x + 1} - \cos\frac{\pi k}{n_y + 1}\right) \tag{51}$$

$$(j = 1, \ldots, n_x; \quad k = 1, \ldots, n_y)$$

Similarly for a 3D lattice of $n_x \times n_y \times n_z$ sites the eigenvalues are:

$$\lambda_{jkl} = -\frac{1}{3\tau}\left(3 - \cos\frac{\pi j}{n_x + 1} - \cos\frac{\pi k}{n_y + 1} - \cos\frac{\pi l}{n_z + 1}\right) \tag{52}$$

$$(j = 1, \ldots, n_x; \quad k = 1, \ldots, n_y; \quad l = 1, \ldots, n_z)$$

These expressions are very similar to (43), but yield substantially different eigenvalue densities. As it is shown in appendix B, the 2D square lattice leads to an eigenvalue density which is very nearly flat near the origin, and therefore the resulting PSD has a $1/f$ shape, while the PSD for the 3D cubic lattice has a $1/f^{0.5}$ shape, and thus models with nearest neighbor interactions yield different behaviors for different lattice dimensions. It is also clear that as one of the sides of, e.g., the 3D lattice is reduced, the eigenvalue density changes

and approaches the eigenvalue density of the 2D lattice (the new density, though, is only proportional to, and not equal to the density for the 2D lattice, because the limiting form of the 3D lattice allows the random walkers to jump out of the lattice at each lattice site, and not just along the sides of the 2D lattice). Therefore lattices with arbitrary sides interpolate between the 1D, 2D and 3D lattices.

Before concluding this section I wish to discuss the role of transport in a model with nearest neighbor interactions, as it was introduced at the end of section II. Formula (43) becomes:

$$\lambda_m = -\frac{1}{\tau}\left(1 - \sqrt{4pq}\cos\frac{\pi m}{n+1}\right) \qquad (m = 1,\ldots,n). \tag{53}$$

The product $4pq$ attains its maximum value 1 when $p = q = 1/2$ and decreases whenever there is drift, therefore transport has the effect of "compressing" the whole eigenvalue distribution about its middle value $1/\tau$, and as either p or q increases the PSD changes more and more to the simple $1/(\omega^2 + \lambda^2)$ shape. It seems that transport does more harm than good and takes us away from a $1/f$ shape, however physical systems that are known to display $1/f$ noise usually are *not* one-dimensional. So it makes sense to consider again the 2D and 3D lattices introduced above, and after some straightforward but tedious calculations one finds that the eigenvalues are

$$\lambda_{jk} = -\frac{1}{2\tau}\left[2 - \cos\frac{\pi j}{n_x + 1} - \sqrt{4pq}\cos\frac{\pi k}{n_y + 1}\right] \tag{54}$$

$$(j = 1,\ldots,n_x; \quad k = 1,\ldots,n_y)$$

for the 2D lattice with transport along y, and

$$\lambda_{jkl} = -\frac{1}{3\tau}\left[3 - \cos\frac{\pi j}{n_x + 1} - \cos\frac{\pi k}{n_y + 1} - \sqrt{4pq}\cos\frac{\pi l}{n_z + 1}\right] \tag{55}$$

$$(j = 1,\ldots,n_x; \quad k = 1,\ldots,n_y; \quad l = 1,\ldots,n_z)$$

for the 3D lattice with transport along z, so that in these cases the PSD should have a $1/f^\alpha$ shape with α between 1 and 1.5 for the 2D lattice and between 0.5 and 1 for the 3D

lattice.

The overall picture is satisfactory but still incomplete, because when dealing with $1/f$ noise we also have to consider current, i.e. transport, noise, and the lattices described above do not really represent reasonable transport channels. Better models of transport channels are developed in the next section.

VI. CONDUCTANCE FLUCTUATIONS

The previous sections of this paper have a mathematical flavor and the results are very general, however it is clear that the main purpose of any theory of $1/f^\alpha$ noise is that of "explaining" its occurrence in resistors. In a limited sense, this is the purpose of this section: I take the diffusion and transport model outlined in section II as a model of charge transport, so that the charge carriers correspond to the individual random walkers of that section, and at the end I derive a Hooge formula for conductance fluctuations.

I define a 3D transport channel as a simple cubic lattice of $n = n_x \times n_y \times n_z$ sites (so that each site is labeled by three indices i, j, k), with drift along the z direction, and with two "interfaces" at $k = 1$ and $k = n_z$ (1D and 2D channels, i.e. "wires" and "strips" are obtained by setting $n_x = n_y = 1$ and $n_y = 1$ respectively). Charge is exchanged only at these interfaces, and here the transport channel may both lose and gain charge. With the labeling defined above, the matrix elements of A for a 3D transport channel are:

$$a_{ijk;ijk} = -1/\tau; \quad (1 < i < n_x, 1 < j < n_y)$$

$$a_{1jk;1jk} = a_{n_xjk;n_xjk} = -5/6\tau; \quad (1 < j < n_y)$$

$$a_{i1k;i1k} = a_{in_yk;in_yk} = -5/6\tau; \quad (1 < i < n_x)$$

$$a_{11k;11k} = a_{1n_yk;1n_yk} = a_{n_x1k;n_x1k} = a_{n_xn_yk;n_xn_yk} = -4/6\tau; \tag{56}$$

$$a_{ij,k+1;ijk} = p/3\tau; \quad a_{ij,k-1;ijk} = q/3\tau;$$

$$a_{i\pm1,jk;ijk} = a_{i,j\pm1,k;ijk} = 1/6\tau;$$

$$a_{ijk,rst} = 0; \quad \text{(all remaining matrix elements)}$$

18

where p and q have the same meaning as in section II. These matrix elements mean that the transition rates to neighbors are the same for every site of the lattice, and that the relaxation times are also the same for all sites in the bulk and on the interfaces, while they change slightly for sites on the boundary (the matrix elements for the 2D channel are very similar). The eigenvalues corresponding to these matrices are:

$$\lambda_{jk} = -\frac{1}{2\tau}\left[2 - \cos\frac{\pi j}{n_x} - \sqrt{4pq}\cos\frac{\pi k}{n_y+1}\right] \tag{57}$$

$$(j = 0, \ldots, n_x - 1; \quad k = 1, \ldots, n_y)$$

for the 2D transport channel with transport along y, and

$$\lambda_{jkl} = -\frac{1}{3\tau}\left[3 - \cos\frac{\pi j}{n_x} - \cos\frac{\pi k}{n_y} - \sqrt{4pq}\cos\frac{\pi l}{n_z+1}\right] \tag{58}$$

$$(j = 0, \ldots, n_x - 1; \quad k = 0, \ldots, n_y - 1; \quad l = 1, \ldots, n_z)$$

for the 3D transport channel with transport along z.

Notice that if d is the lattice dimension, δ is the lattice spacing, $p \approx q \approx 0.5$ and $L = n_z\delta$ is the channel length, the smallest eigenfrequency is $|\lambda_{max}| \approx \frac{\pi^2}{2dn_z^2\tau}$, and since $\tau = \frac{\delta^2}{D}$, then $|\lambda_{max}| \approx \frac{\pi^2 D}{2dL^2}$. The diffusion time $|\lambda_{max}|^{-1}$ is approximately the average lifetime of the longest lived transient (see eq. 40), therefore if there is no source, this is also the average time needed to empty the transport channel. However it is also clear that if the contacts to the "outside" have a cross-section which is smaller than the cross-section of the transport channel, then $|\lambda_{max}|$ becomes smaller (i.e. it takes longer to empty the channel). Indeed the limiting case of a transport channel with no input-output (and no drift) has eigenvalues

$$\lambda_{jkl} = -\frac{1}{3\tau}\left[3 - \cos\frac{\pi j}{n_x} - \cos\frac{\pi k}{n_y} - \cos\frac{\pi l}{n_z}\right] \tag{59}$$

$$(j = 0, \ldots, n_x - 1; \quad k = 0, \ldots, n_y - 1; \quad l = 0, \ldots, n_z - 1)$$

and $|\lambda_{max}| = 0$. This is something that we already knew from section IV, however equations (58) and (59) show that the eigenvalues do not change appreciably when one

19

shuts down the channel, while the diffusion time $|\lambda_{max}|^{-1}$ becomes much larger than the previously estimated $\frac{\pi^2 D}{2dL^2}$, thereby increasing the range of the $1/f^\alpha$ region.

The PSD's can be computed from (57) and (58) and they have the same general behavior as the 2D and 3D lattices discussed in the previous section: examples are shown in figures 8 and 9. Figure 10 shows a simulated signal for the 2D channel.

I assume a noisy source of charge at each end of the transport channel, and for given noise rates, it is easy to compute the equilibrium values $\langle N_{ijk} \rangle_{eq}$: if the noise source at the "entrance" of the transport channel has an average rate $p\nu_0$ and the noise source at the "exit" has an average rate $q\nu_0$, then all the sites have the same equilibrium population $\langle N \rangle_{eq} = \langle N_{ijk} \rangle_{eq} = \tau\nu_0$, and the environment is uniform (figure 11 illustrates this point for a 1D chain). This is especially important if the model is to represent a resistor, because it means that on the average the charge density is the same over the whole transport channel, i.e. there are no space charge effects. At the same time this requirement satisfies the uniformity hypothesis that was used to find the PSD.

A rough approximation of the current PSD can now be obtained as follows. The net flow of charge carriers across any section of the transport channel (number of carriers per unit time) is given by

$$\text{flow across k-th section} = \sum_{\substack{i=1,n_x \\ j=1,n_y}} \left(\frac{p}{\tau} N_{i,j,k} - \frac{q}{\tau} N_{i,j,k+1} \right) \approx \frac{(p-q)}{\tau} \sum_{\substack{i=1,n_x \\ j=1,n_y}} N_{i,j,k} \qquad (60)$$

$$= \frac{(p-q)}{\tau} (n_x n_y) N_k = \frac{Av}{\delta^3} N_k \qquad (61)$$

and therefore the electric current is:

$$I \approx I_k = \frac{Aev}{\delta^3} N_k \qquad (62)$$

where δ is the lattice spacing, $v = (p-q)\frac{\delta}{\tau}$ is the drift speed, $A = n_x n_y \delta^2$ is the cross-section of the transport channel, e is the charge of each carrier, and $N_k = \frac{1}{n_x n_y} \sum_{i,j} N_{i,j,k}$. Now let $S(\omega)$ be the PSD of the fluctuations of the number of charge carriers averaged over the channel section, and S_I be the PSD of the electric current I, then $\langle I \rangle = \frac{Aev}{\delta^3} \langle N \rangle_{eq}$, and

$$S_I(\omega) \approx \left(\frac{Aev}{\delta^3}\right)^2 S(\omega) \tag{63}$$

$$\approx \frac{\langle I \rangle^2}{\langle N \rangle_{eq}^2} \frac{\sigma^2}{2\pi} \int_{|\lambda_{min}|}^{|\lambda_{max}|} \frac{f_A(|\lambda|)}{\omega^2 + |\lambda|^2} d|\lambda| \tag{64}$$

$$\approx \frac{\langle I \rangle^2}{2\pi\tau \langle N \rangle_{eq}} \int_{|\lambda_{min}|}^{|\lambda_{max}|} \frac{f_A(|\lambda|)}{\omega^2 + |\lambda|^2} d|\lambda|, \tag{65}$$

where $\sigma^2 \approx 2\langle N \rangle_{eq}/\tau$ has been used. Now notice that the integral in (65) approaches the value $\frac{1}{n}\sum_{k=1}^{n} \frac{1}{|\lambda_k|^2}$ as $\omega \approx |\lambda_{max}|$, and if $n \gg 1$, λ_{max} is very small and $\frac{1}{n}\sum_{k=1}^{n} \frac{1}{|\lambda_k|^2} \approx \frac{1}{n}\frac{1}{|\lambda_{max}|^2}$. Therefore, in the range $|\lambda_{min}| < \omega < |\lambda_{max}|$, the integral in (65) is approximately equal to $\frac{1}{n|\lambda_{max}|^2}\left(\frac{|\lambda_{max}|}{\omega}\right)^\alpha$, and then

$$\frac{S_I(\omega)}{\langle I \rangle^2} \approx \frac{1}{2\pi\tau n \langle N \rangle_{eq} |\lambda_{max}|^2}\left(\frac{|\lambda_{max}|}{\omega}\right)^\alpha = \left(\frac{1}{2\pi\tau |\lambda_{max}|^2}\right)\frac{1}{N_{tot}}\left(\frac{|\lambda_{max}|}{\omega}\right)^\alpha, \tag{66}$$

where $N_{tot} = n\langle N \rangle_{eq}$ is the total number of charge carriers in the channel. Now remember that if G is the conductance then $S_I(\omega)/\langle I \rangle^2 = S_G(\omega)/\langle G \rangle^2$ and therefore equation (66) gives the PSD of conductance fluctuations as well, and corresponds to the Hooge formula [17]. In view of the previous discussion on λ_{max}, it is clear that the coefficient in front of the $N_{tot}^{-1}\omega^{-\alpha}$ dependence has no fundamental significance.

VII. CONCLUSIONS

I have described a mathematical mechanism whereby flicker noise appears as a natural feature of a collection of identical interacting relaxing systems driven by white noise. The first and most prominent feature of the mechanism studied in this paper is that generic PSD's for diffusion processes should be of the form $1/f^\alpha$ with $0.5 < \alpha < 1.5$ and that $\alpha = 1$ has no special significance, apart from the fact that nearly all the observed systems are approximately 2-dimensional, and $\alpha = 1$ is exactly what one should expect from the simple diffusion model for a 2D system (indeed experiments observe a whole range of values of α in the vicinity of 1, see the list of α values in [5]). An important consequence of the linearity of the model is that stationarity and Gaussianity - actually observed in experiments - do both arise naturally.

21

I wish to emphasize the universal features of the model: it applies whenever there are relaxing linear systems, and diffusion and transport are just special cases. The linearity of the model also has an appealing simplicity that nonlinear models certainly lack. Given the probabilistic nature of the interaction between different sites, noise is self-generated by the system, and there is no real need of an external noise source.

It may seem that the validity of the model is limited by the request that the populations be very large: but this was only used to make the noise source Gaussian. Another seemingly unnatural assumption is that each random-walker may step to other sites only at given, discrete, times. Both problems can be fixed by assuming that each random-walker jumps to adjacent sites with an exponential waiting time distribution, so that now the relaxation time τ must be regarded as the average transition time. It is very easy to see that this leads to exactly the same differential equations for the average values. Moreover the number of transitions during any give time interval must be a Poissonian deviate. Very high frequencies mean short times and small averages, so that at high frequencies the discrete character of the number fluctuations is very prominent, and it leads to shot noise. Lower frequencies mean longer times and therefore Poisson distributions with bigger average values. It is well-known that the greater the average, the more the Poisson distribution resembles the Gaussian, therefore at low frequency the driving noise is just plain white Gaussian noise, and once again the mathematics of this paper is valid and applicable as it is.

It was remarked in the introduction that other diffusion theories exist, but they all fail in some respect. In particular the thermal diffusion theory of Voss and Clark [9] was troubled after its appearance by several problems (listed in [17]), and especially by the lack of spatial correlations. Though at the beginning there appeared to be some correlations, they were not found by later experiments (see, e.g. [18]). As in *any* diffusion theory, spatial correlation must be present also in the treatment of this paper. However none of the experiments that ruled out the Voss and Clark model applies here. This important point is discussed in appendix C.

I wish to point out that the theory also explains, at least qualitatively, some other facts like the steepening of the PSD observed at low temperatures by Voss and Clark [9] and by Eberhard and Horn [19]. In fact the difference $(p - q)$ is related to the current flowing in the sample by

$$(p - q) = \frac{I\tau}{A\rho\delta} \tag{67}$$

(ρ is the charge density), therefore, if the current is held fixed while the temperature is lowered, the difference $(p - q)$ increases since the relaxation time τ also increases. Then the factor $\sqrt{4pq} = \sqrt{1 - (p - q)^2}$ decreases and the eigenvalues (whatever the dimensionality of the lattice) are compressed about their average value, and the PSD becomes steeper.

APPENDIX A

If all the random-walkers see the same average environment we may define an average $\langle |F|^2 \rangle$, and use formula (16) to obtain

$$\langle |F|^2 \rangle \approx \frac{1}{n} \langle \sum_{j=1}^{n} |F_j|^2 \rangle \tag{A1}$$

$$= \frac{1}{n} \langle F^+ \cdot F \rangle \tag{A2}$$

$$= \frac{1}{n} \left\langle f^+ \left[(i\omega \mathbb{1} - A)^{-1} \right]^+ \cdot \left[(i\omega \mathbb{1} - A)^{-1} \right] f \right\rangle \tag{A3}$$

$$= \frac{1}{n} \left\langle \sum_{j,k,l} f_j^* \left[(i\omega \mathbb{1} - A)^{-1} \right]_{jk}^+ \left[(i\omega \mathbb{1} - A)^{-1} \right]_{kl} f_l \right\rangle \tag{A4}$$

$$= \frac{1}{n} \sum_{j,l} \left\{ \left[(i\omega \mathbb{1} - A)^{-1} \right]^+ \cdot \left[(i\omega \mathbb{1} - A)^{-1} \right] \right\}_{jl} \langle f_j^* f_l \rangle. \tag{A5}$$

If we make make use of the assumptions of independence of the noise processes and of average environment uniformity:

$$\langle |F|^2 \rangle \approx \frac{1}{n} \sum_{j,l} \left\{ \left[(i\omega \mathbb{1} - A)^{-1} \right]^+ \cdot \left[(i\omega \mathbb{1} - A)^{-1} \right] \right\}_{jl} \delta_{jl} \langle |f_l|^2 \rangle \tag{A6}$$

$$= \frac{1}{n} \langle |f|^2 \rangle Trace \left\{ \left[(i\omega \mathbb{1} - A)^{-1} \right]^+ \cdot \left[(i\omega \mathbb{1} - A)^{-1} \right] \right\}. \tag{A7}$$

The relaxation matrices A that we consider in this paper are real matrices. Since they are nonsingular they are certainly diagonalizable, unless there are degenerate eigenvalues

23

such that they can only be put in a Jordan quasidiagonal form. However in a physical environment the degeneracy is likely to be removed by any small randomness in the matrix elements. This does not affect substantially the shape of the PSD, because the eigenvalue spectrum is stable against small perturbations (see section 6.3 in [13]). Now let $\boldsymbol{\eta}$ be an eigenvector of A, so that $A\boldsymbol{\eta} = \lambda\boldsymbol{\eta}$, then $\boldsymbol{\eta}^+$ is a left eigenvector of A^t with eigenvalue λ^*, i.e. $\boldsymbol{\eta}^+ A^t = \lambda^*\boldsymbol{\eta}$ (see [13] for the algebra of left and right eigenvectors). If we take normalized left and right eigenvectors, i.e. $\boldsymbol{\eta}_j^+ \boldsymbol{\eta}_k = \delta_{jk}$, equation (A7) can also be written as

$$\langle |F|^2 \rangle \approx \frac{1}{n} \langle |f|^2 \rangle \sum_{j,l} \boldsymbol{\eta}_j^+ \left[(i\omega\mathbb{1} - A)^{-1} \right]^+ \cdot \left[(i\omega\mathbb{1} - A)^{-1} \right] \boldsymbol{\eta}_l \tag{A8}$$

$$= \frac{1}{n} \langle |f|^2 \rangle \sum_{j=1}^n \frac{1}{-i\omega - \lambda_j^*} \frac{1}{i\omega - \lambda_j} \tag{A9}$$

$$= \frac{1}{n} \langle |f|^2 \rangle \sum_{j=1}^n \frac{1}{\omega^2 + |\lambda_j|^2}, \tag{A10}$$

which is the same as (25) (see also theorem 4.4.3 in [13]). Some information has been lost in this proof, we have not found the individual PSD's for the populations at each site, but rather an average PSD. However something else has been gained, now the proof has been extended to incorporate non-symmetrical matrices; this means that the results of section III hold for the symmetrical case of diffusion as well as for the non-symmetrical case of transport.

APPENDIX B

Take a set of eigenvalues $\{\lambda_m\}_{m=1,\dots,n}$ such that $\lambda_m \propto m^2$ for small m, so that for large n, $\lambda(t) \approx \alpha t^2$ and one has to compute the integral

$$\int_{\lambda_{min}}^{\lambda_{max}} \frac{dt}{\omega^2 + \alpha^2 t^4}, \tag{B1}$$

to find the PSD. The result of the indefinite integration is

$$\frac{1}{2\sqrt{2|\alpha|}\omega^{3/2}} \left[\arctan\left(1 + t\sqrt{\frac{2|\alpha|}{\omega}} \right) - \arctan\left(1 - t\sqrt{\frac{2|\alpha|}{\omega}} \right) \right] +$$

$$+ \frac{1}{4\sqrt{2|\alpha|}\omega^{3/2}} \log\left(\frac{|\alpha|t^2 + t\sqrt{2|\alpha|\omega} + \omega}{|\alpha|t^2 - t\sqrt{2|\alpha|\omega} + \omega} \right), \tag{B2}$$

24

and thus for $\lambda_{min} \ll \omega \ll \lambda_{max}$

$$\int_{\lambda_{min}}^{\lambda_{max}} \frac{dt}{\omega^2 + \alpha^2 t^4} \approx \frac{\pi}{2\sqrt{2|\alpha|}} \frac{1}{\omega^{3/2}}. \tag{B3}$$

In the case of the 1D chain discussed in section V, $\lambda_m = -\frac{1}{\tau}\left(1 - \cos\frac{\pi m}{n+1}\right) \approx -\frac{\pi^2 m^2}{2\tau n^2}$ for $m \ll n$, $n \gg 1$, and indeed integrating the full expression one finds that

$$\int_{\lambda_{min}}^{\lambda_{max}} \frac{dt}{\omega^2 + \lambda^2} \propto \frac{1}{\omega^{1.5}} \tag{B4}$$

for $\lambda_{min} \ll \omega \ll \lambda_{max}$. Similarly, for the 2D lattice one finds that the eigenvalues (51) can be approximated by the expression $|\lambda_{jk}| \approx \frac{\pi^2 j^2}{4\tau n_x^2} + \frac{\pi^2 k^2}{4\tau n_y^2}$, and if $n_x = n_y = n_s$, $n_s \gg 1$, and $j, k \ll n_s$, then the sum in (26) becomes

$$\sum_{m=1}^{n} \frac{1}{\omega^2 + \lambda_m^2} = \sum_{j,k=1}^{n_s} \frac{1}{\omega^2 + \lambda_{jk}^2} \tag{B5}$$

$$\approx \int_{1/n_s}^{1-1/n_s} \int_{1/n_s}^{1-1/n_s} \frac{dxdy}{\omega^2 + \left(\frac{\pi^2 r^2}{4\tau}\right)^2} \tag{B6}$$

$$\approx \frac{\pi}{2} \int_{\sqrt{2}/n_s}^{\sqrt{\xi}} \frac{rdr}{\omega^2 + \left(\frac{\pi^2 r^2}{4\tau}\right)^2} \tag{B7}$$

$$\approx \frac{\pi}{4} \int_{2/n_s^2}^{\xi} \frac{dt}{\omega^2 + \left(\frac{\pi^2}{4\tau}\right)^2 t^2}, \tag{B8}$$

where $\frac{j}{n_s} \to x$, $\frac{k}{n_s} \to y$, $r^2 = x^2 + y^2$, and ξ is a number between 1 and 2 (and therefore $\xi \gg \frac{2}{n_s^2}$). The integral (B8) is just the integral (1) that leads to a $1/f$ PSD. All this can be repeated for the 3D lattice using (52), and one finds that $|\lambda_{jkl}| \approx \frac{\pi^2 j^2}{6\tau n_x^2} + \frac{\pi^2 k^2}{6\tau n_y^2} + \frac{\pi^2 l^2}{6\tau n_z^2}$, and if $n_x = n_y = n_z = n_s$, $n_s \gg 1$, and $j, k, l \ll n_s$, then the sum in (26) becomes

$$\sum_{m=1}^{n} \frac{1}{\omega^2 + \lambda_m^2} = \sum_{j,k,l=1}^{n_s} \frac{1}{\omega^2 + \lambda_{jkl}^2} \tag{B9}$$

$$\approx \int_{1/n_s}^{1-1/n_s} \int_{1/n_s}^{1-1/n_s} \int_{1/n_s}^{1-1/n_s} \frac{dxdydz}{\omega^2 + \left(\frac{\pi^2 r^2}{6\tau}\right)^2} \tag{B10}$$

$$\approx \frac{\pi}{2} \int_{\sqrt{3}/n_s}^{\sqrt{\xi}} \frac{r^2 dr}{\omega^2 + \left(\frac{\pi^2}{6\tau}\right)^2 r^4} \tag{B11}$$

$$\approx \frac{9\tau}{2\pi} \sqrt{\frac{\tau}{3}} \frac{1}{\omega^{1/2}}, \tag{B12}$$

where, once again, $\frac{j}{n_s} \to x$, $\frac{k}{n_s} \to y$, $\frac{l}{n_s} \to z$, $r^2 = x^2 + y^2 + z^2$, $1 < \xi < 3$, and $\lambda_{min} \ll \omega \ll \lambda_{max}$. The sum (B9) thus gives a $1/f^{0.5}$ PSD.

APPENDIX C

The space correlation function is easily computed using the formalism of section III

$$\langle (N_j^*(t) - \langle N_j \rangle_{eq}^*)(N_k(t) - \langle N_k \rangle_{eq}) \rangle = \frac{1}{(2\pi)^2} \int_{-\infty}^{+\infty} \int_{-\infty}^{+\infty} d\omega d\omega' e^{-i(\omega-\omega')t} \langle F_j^*(\omega)F_k(\omega') \rangle \quad \text{(C1)}$$

so that, using (22) and $\langle \gamma_l^*(\omega)\gamma_m(\omega') = \sigma^2 \delta_{lm}\delta(\omega - \omega')$

$$\langle F_j^*(\omega)F_k(\omega') \rangle = \sigma^2 \sum_{l=1}^{n} \frac{(\eta_l^*)_j(\eta_l)_k}{\omega^2 - |\lambda_l|^2} \delta(\omega - \omega'), \quad \text{(C2)}$$

and thus the integral (C1) becomes

$$\langle (N_j^*(t) - \langle N_j \rangle_{eq}^*)(N_k(t) - \langle N_k \rangle_{eq}) \rangle = \frac{\sigma^2}{(2\pi)^2} \int_{-\infty}^{+\infty} d\omega \sum_{l=1}^{n} \frac{(\eta_l^*)_j(\eta_l)_k}{\omega^2 - |\lambda_l|^2} = \frac{\sigma^2}{4\pi} \sum_{l=1}^{n} \frac{(\eta_l^*)_j(\eta_l)_k}{|\lambda_l|}.$$

$$\text{(C3)}$$

In general the sum (C3) is different from zero, however this space correlation is not ruled out by past experiments. I review now the arguments of a few of them [20–23].

The experiment reported in [20] simply does not apply here, since it ruled out correlations in two gold films that were in thermal contact but electrically disconnected .

The authors of [21] tried to measure voltage cross correlations in a thin wire that was etched, together with the contact pads, from a thin metal film. I argue here that they did not observe fluctuations *in the wire* but rather *in each pad separately*. In fact whatever the (microscopic) origin of the fluctuations it must act in the pads as well as in the wire. If the explanation proposed in this paper has any validity at all, one should then expect the whole "wire + pads" system to behave - more or less - like a 2D system, and indeed what they observe is not the $1/f^{1.5}$ spectrum that was expected from the Voss and Clark theory, but a $1/f$ spectrum which is characteristic of a 2D system (see figure 2 in [21]).

Again, the experiments reported in [22,23] test thermal fluctuations and do not apply here.

26

Furthermore the observed dependence of noise power on sample width, that the authors of those papers used to argue that the noise arises from fluctuations in the local sheet resistivity, does not apply to number fluctuations and can be used instead to support formula (66), which does predict the observed dependence.

REFERENCES

[1] W. H. Press, Comments Astrophys. **7**, 103 (1978).

[2] B. J. West and M. Shlesinger, Int. J. Mod. Phys. **B3**, 795 (1989); Am. Sci. **78**, 40 (1990).

[3] M. Gardner, Sci. Am. **238**, 16 (1978).

[4] R. F. Voss and J. Clarke, Nature **258**, 317 (1975); J. Acoust. Soc. Am. **63**, 258 (1978).

[5] Sh. M. Kogan, Sov. Phys. Usp. **28**, 170 (1985).

[6] P. Dutta and P. M. Horn, Rev. Mod. Phys. **53**, 497 (1981).

[7] M. B. Weissman, Rev. Mod. Phys. **60**, 537 (1988).

[8] Here a "linear system" is whatever can be described by a set of variables $\boldsymbol{y} = \{y_i\}$ with the evolution equation $\dot{\boldsymbol{y}} = A\boldsymbol{y}$, where A is a real constant matrix. If $\boldsymbol{y}$ is a set of relaxing systems, A shall be called "relaxation matrix".

[9] R. F. Voss and J. Clarke, Phys. Rev. **B13**, 556 (1976).

[10] W. Feller, *An Introduction to Probability Theory and Its Applications*, 3rd revised printing, (Wiley, New York, 1968).

[11] D. R. Cox and H. D. Miller, *The Theory of Stochastic Processes* (Chapman and Hall, London, 1965).

[12] M. C. Wang and G. E. Uhlenbeck, Rev. Mod. Phys. **17**, 323 (1945), also in N. Wax (editor) *Selected Papers on Noise and Stochastic Processes* (Dover, New York, 1955).

[13] R. A. Horn and C. R. Johnson, *Matrix Analysis* (Cambridge University Press, Cambridge, 1987).

[14] F. Brauer and J.A.Nohel *The Qualitative Theory of Ordinary Differential Equations* (Dover, New York, 1989).

[15] This is also clear if we take the sum (26) and use the Wiener-Kintchine theorem to evaluate the variance of the process.

[16] W. H. Press, S. A. Teukolsky, W. T. Vetterling and B. P. Flannery *Numerical Recipes in C, The Art of Scientific Computing, Second Edition* (Cambridge University Press, Cambridge, 1992).

[17] F. N. Hooge, T. G. M. Kleinpenning and L. K. J. Vandamme, Rep. Prog. Phys. **44**, 479 (1981).

[18] J. H. Scofield, J. V. Mantese and W. W. Webb, Phys. Rev. **B32**, 736 (1985).

[19] J. W. Eberhard and P. M. Horn, Phys. Rev. **18**, 6681 (1978).

[20] J. H. Scofield, D. H. Darling and W. W. Webb, Phys. Rev. **B24**, 7450 (1981).

[21] R. D. Black, M. B. Weissman and F. M. Fliegel, Phys. Rev. **B24**, 7454 (1981).

[22] D. M. Fleetwood, J. T. Masden and N. Giordano, Phys. Rev. Lett. **50**, 450 (1983).

[23] J. H. Scofield, J. V. Mantese and W. W. Webb, Phys. Rev. **32**, 736 (1985).
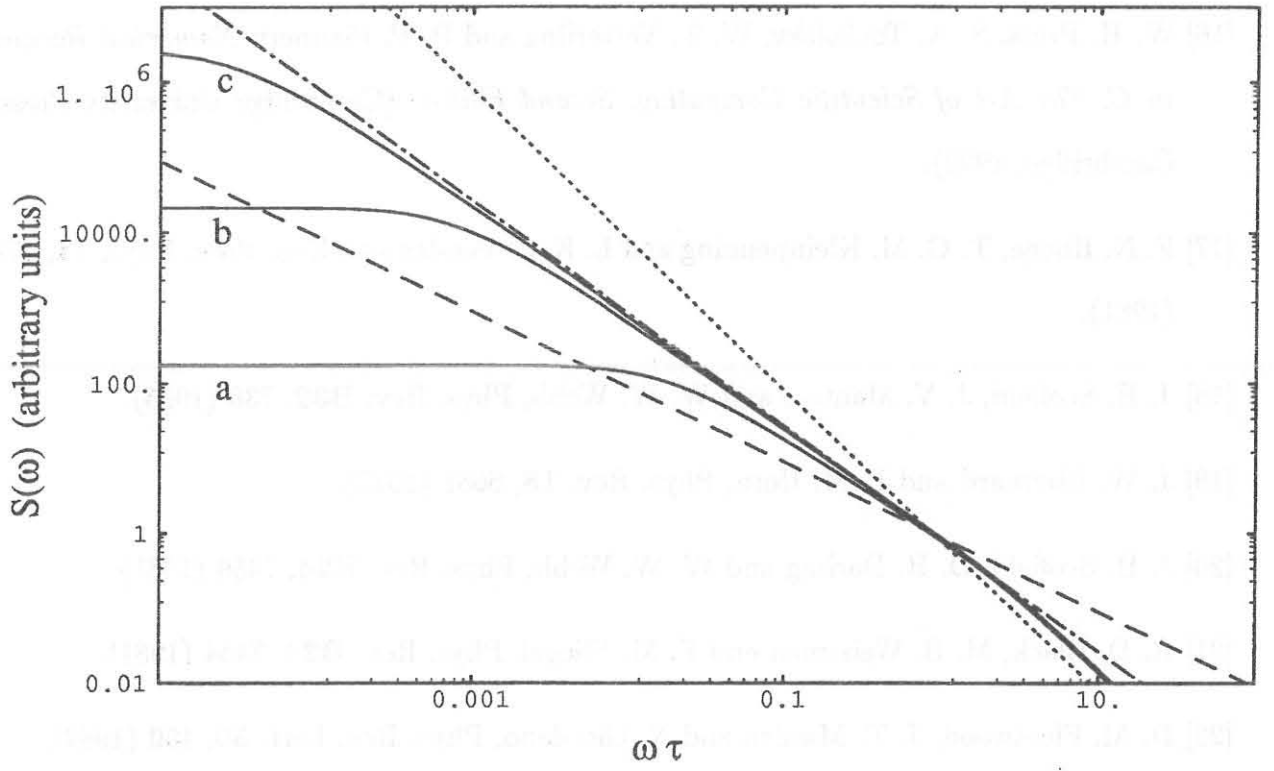
FIG. 1. PSD's for 1D chains of different lengths n calculated using (27). The solid lines show the PSD's for chains with a) $n = 20$, b) $n = 100$, and c) $n = 500$. The straight lines are for reference and represent $1/f^\alpha$ spectra with $\alpha = 1$ (dashed), $\alpha = 1.5$ (dashed-dotted), and $\alpha = 2$ (dotted).
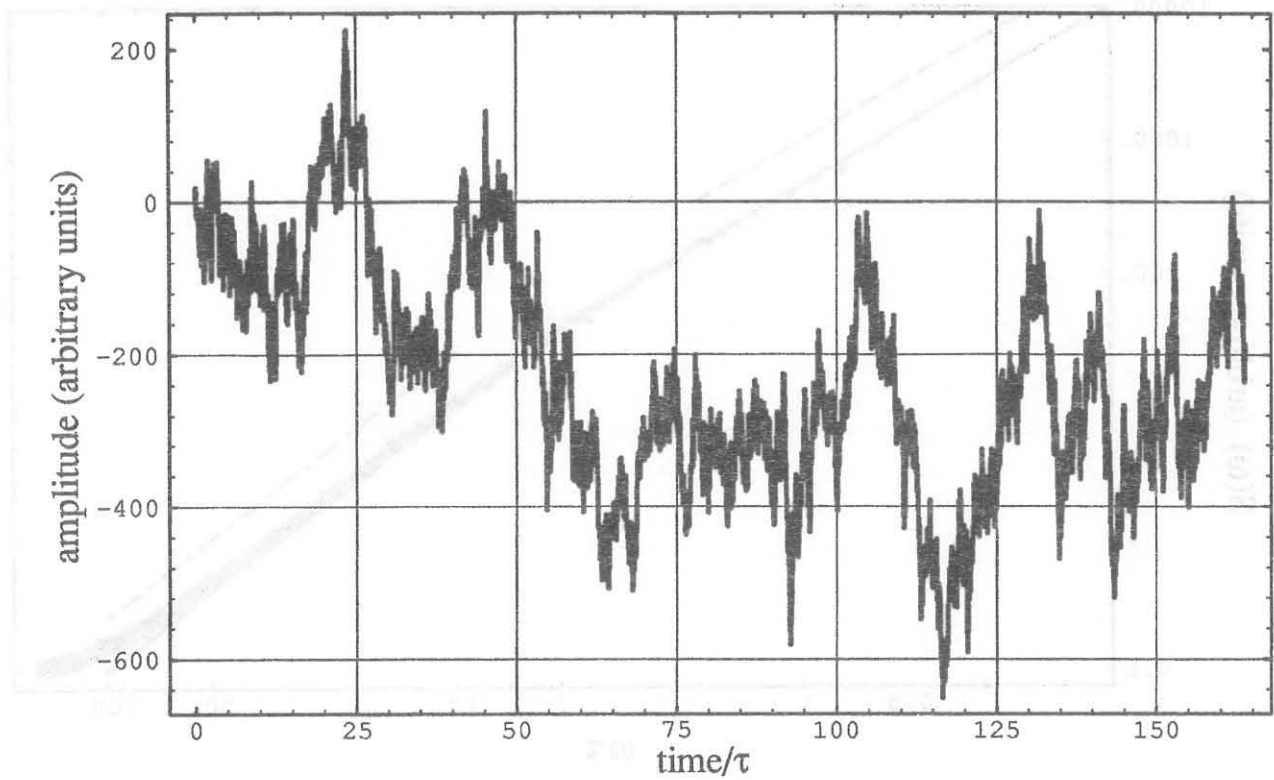
FIG. 2. A small portion (4096 samples) of the simulated signal for a 1D chain with 100 sites and with a noise source at each end of the chain. The signal is the population fluctuation of the middle element (site 50). The relaxation time is $\tau = 0.5$ and the simulation step is $\Delta t = 0.02$ (arbitrary time units).

31
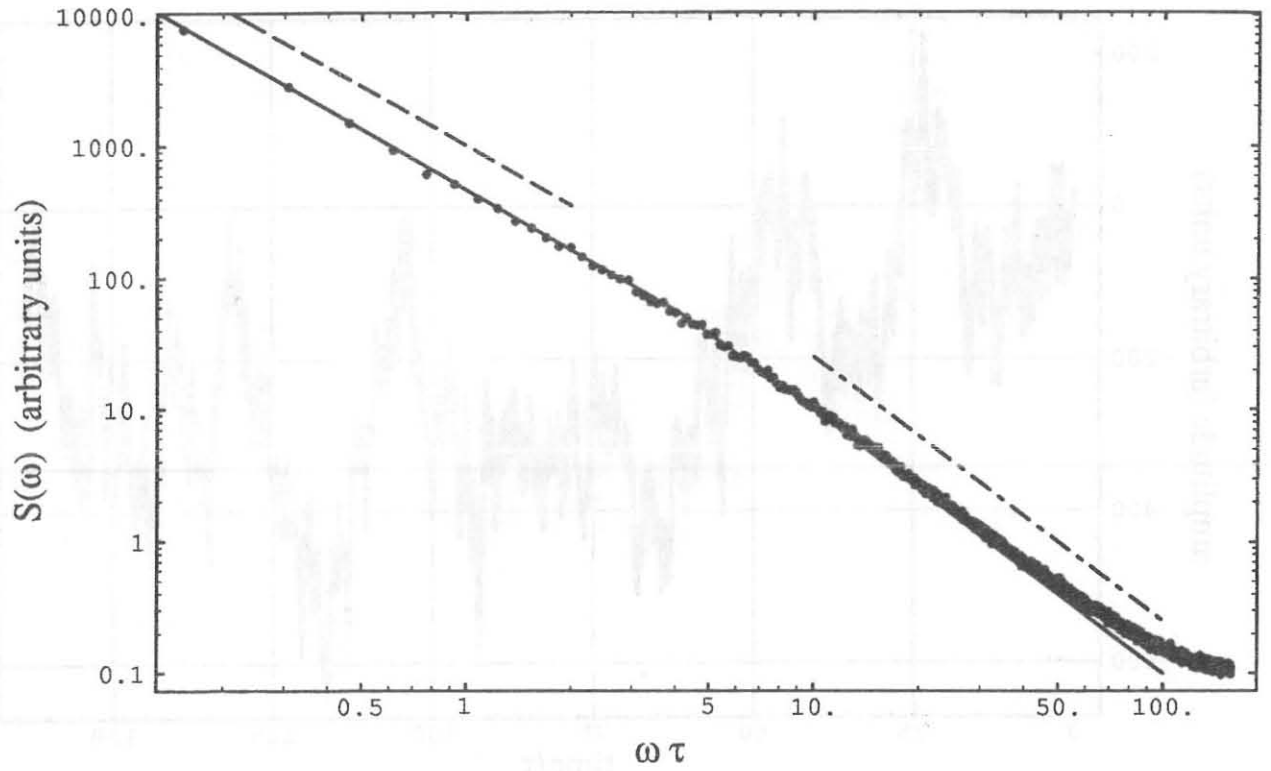
FIG. 3. PSD of the population fluctuations of the middle site (site 50) of a 1D chain of 100 sites and with a noise source at each end of the chain. 2^{20} samples have been generated and each point is the average of 256 PSD estimates obtained from records of 2048 samples each. The relaxation time is $\tau = 0.5$ and the simulation step is $\Delta t = 0.02$ (arbitrary time units).

The solid curve is the theoretical curve b), shown in figure 1). The dashed line shows the slope of a $1/f^{1.5}$ spectrum, while the dashed-dotted line shows the slope of a $1/f^2$ spectrum. The departure from the $1/f^2$ behavior at high frequency is due both to the comparatively large time step and to aliasing.
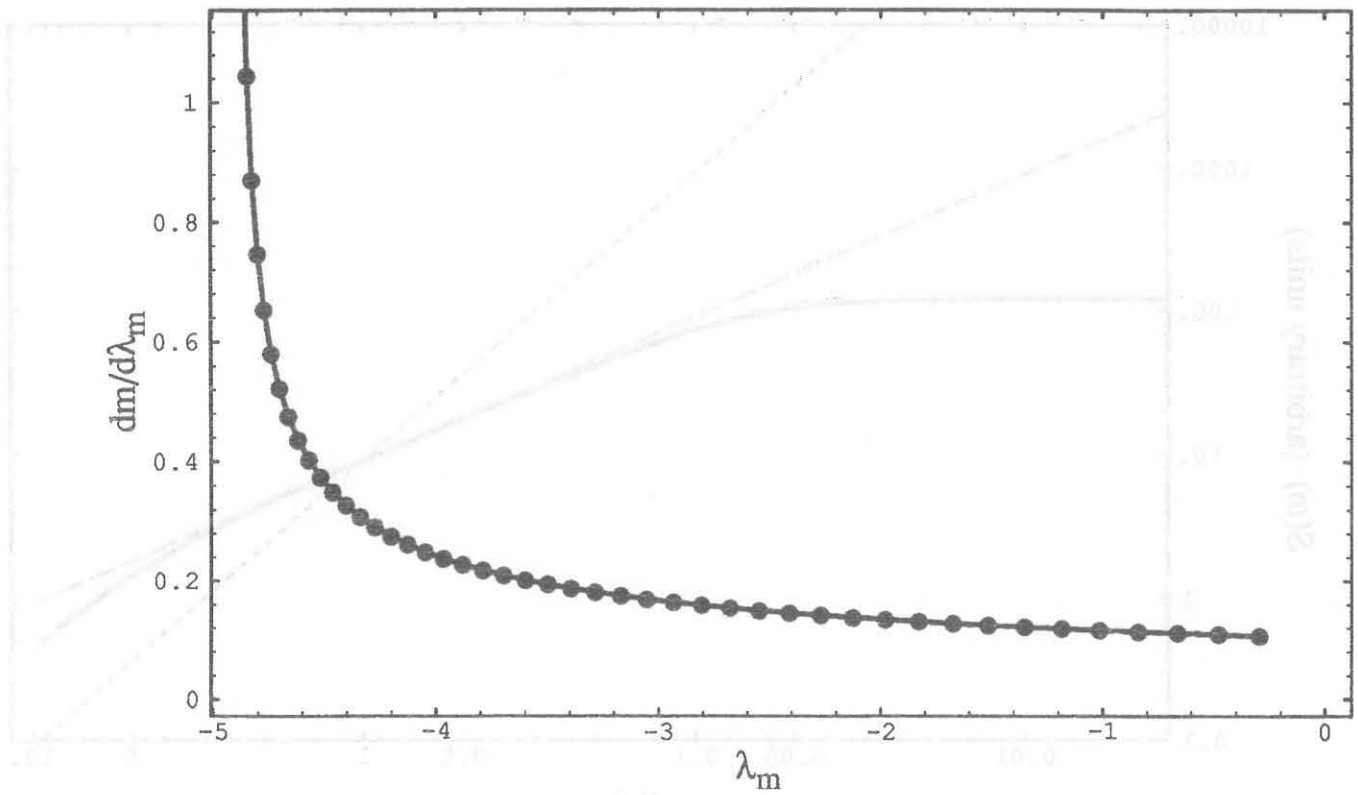
FIG. 4. Eigenvalue density for the 1D chain with matrix elements $a_{jk} = 1/|j - k|^2$ if $j \neq k$, $a_{kk} = -1/\tau = \pi^2/3$, and $n = 50$. The dots show the numerical result (obtained with the Jacobi algorithm, see [13,16]), while the dotted line shows the approximate theoretical curve.
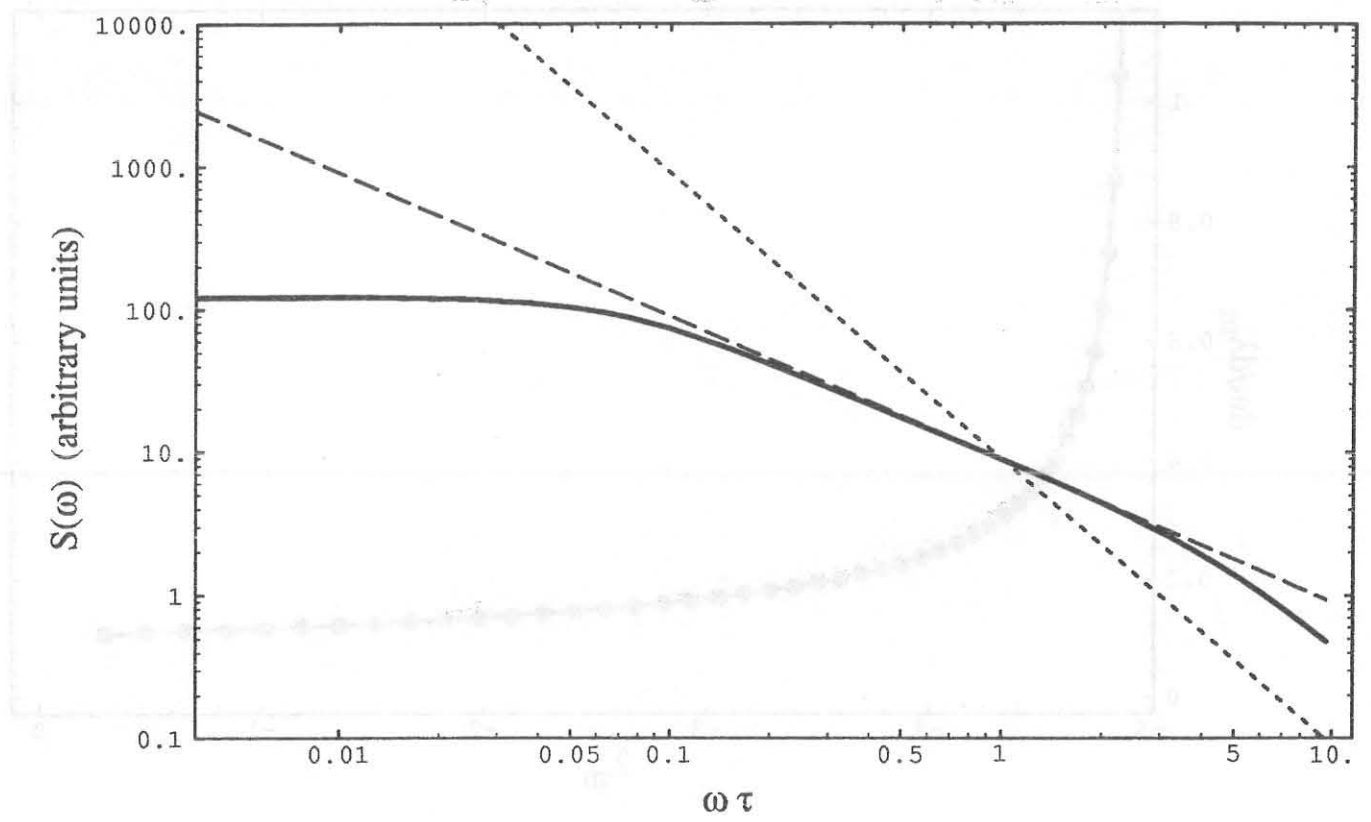
FIG. 5. PSD obtained analytically from the eigenvalue density of figure 4 and from (27). The straight lines are for reference and represent $1/f^\alpha$ spectra with $\alpha = 1$ (dashed), and $\alpha = 2$ (dotted).
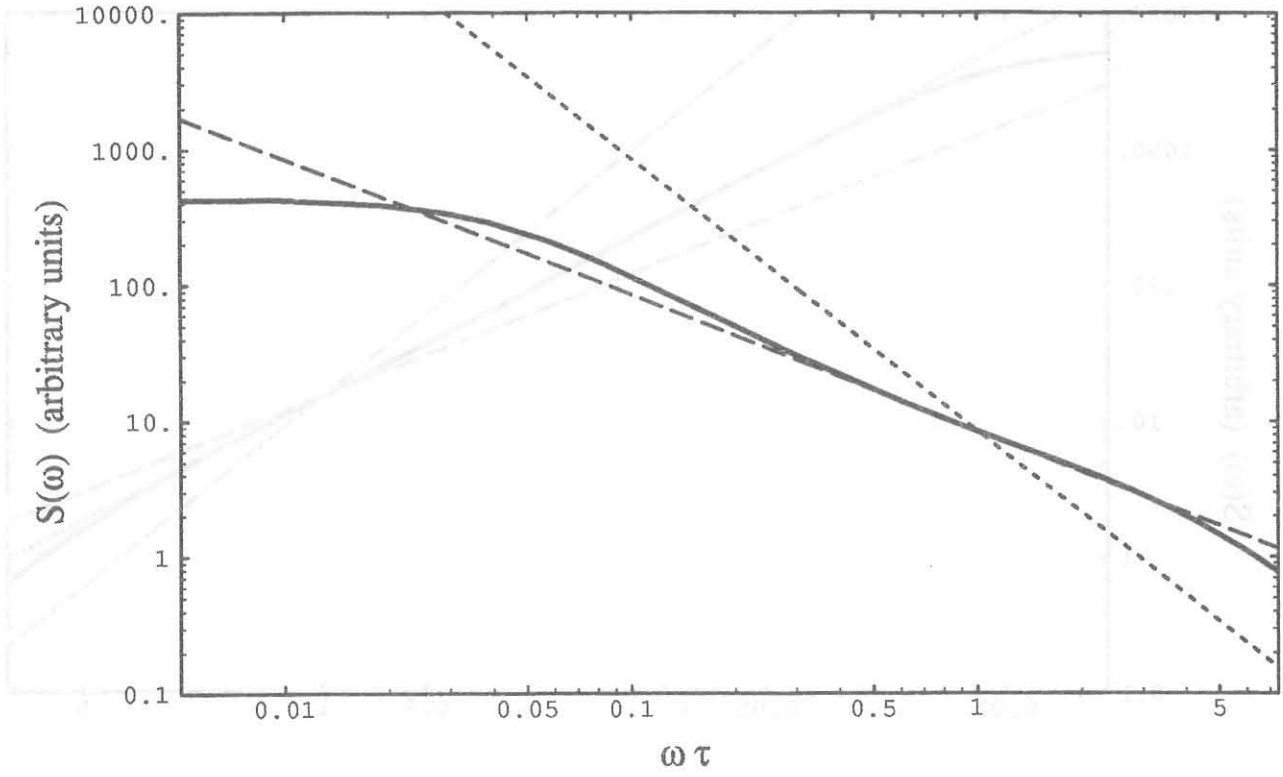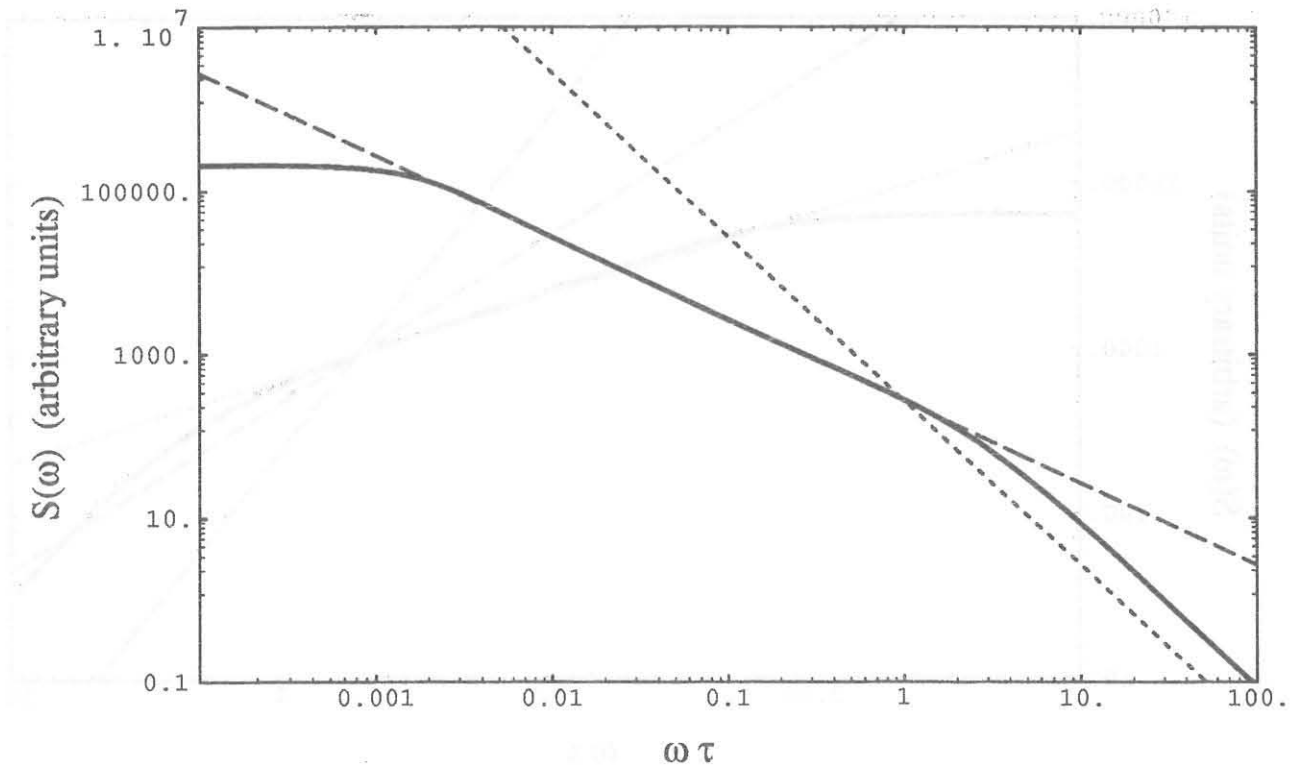
FIG. 6. PSD for the 1D chain with long range $\kappa^{-|j-k|}$ couplings (here $\kappa = 0.6$, $n = 50$). The straight lines are for reference and represent $1/f^\alpha$ spectra with $\alpha = 1$ (dashed), and $\alpha = 2$ (dotted).
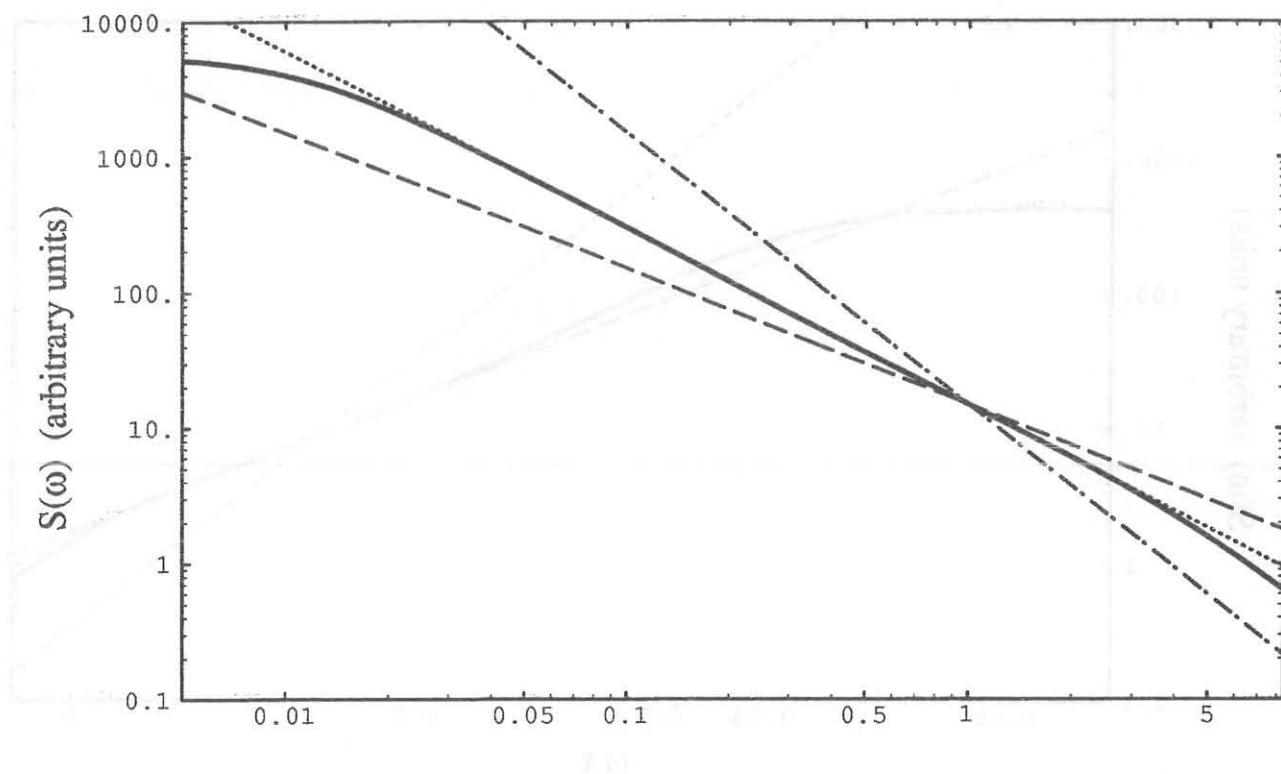
FIG. 7. PSD for the 1D chain with long range $1/|j - k|^3$ couplings (here $n = 50$). The straight lines are for reference and represent $1/f^\alpha$ spectra with $\alpha = 1$ (dashed), $\alpha = 1.3$ (dotted), and $\alpha = 2$ (dashed-dotted).

FIG. 8. PSD for the 2D transport channel ($n_x = 20, n_z = 45$). The straight lines are for reference and represent $1/f^\alpha$ spectra with $\alpha = 1$ (dashed), and $\alpha = 2$ (dotted).
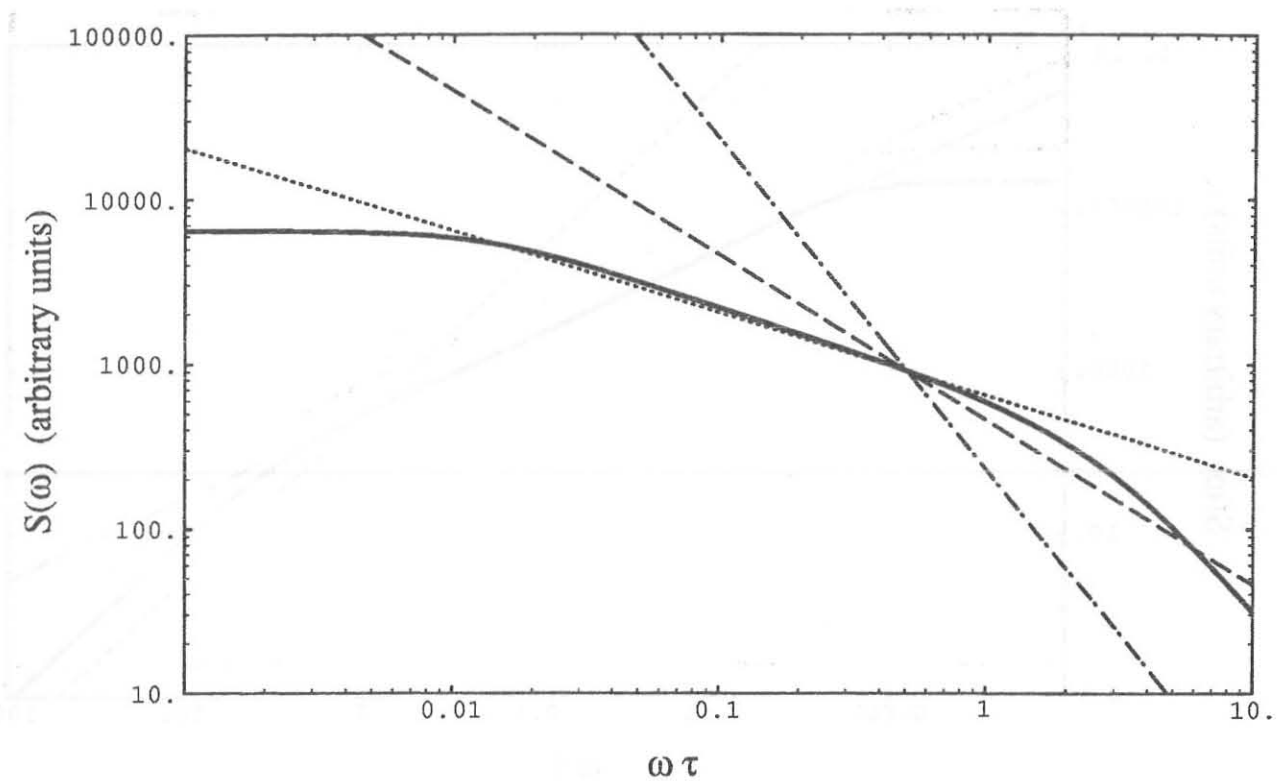
FIG. 9. PSD for the 3D transport channel ($n_x = 15, n_y = 15, n_z = 15$). The straight lines are for reference and represent $1/f^\alpha$ spectra with $\alpha = 1$ (dashed), $\alpha = 0.5$ (dotted), and $\alpha = 2$ (dashed-dotted).
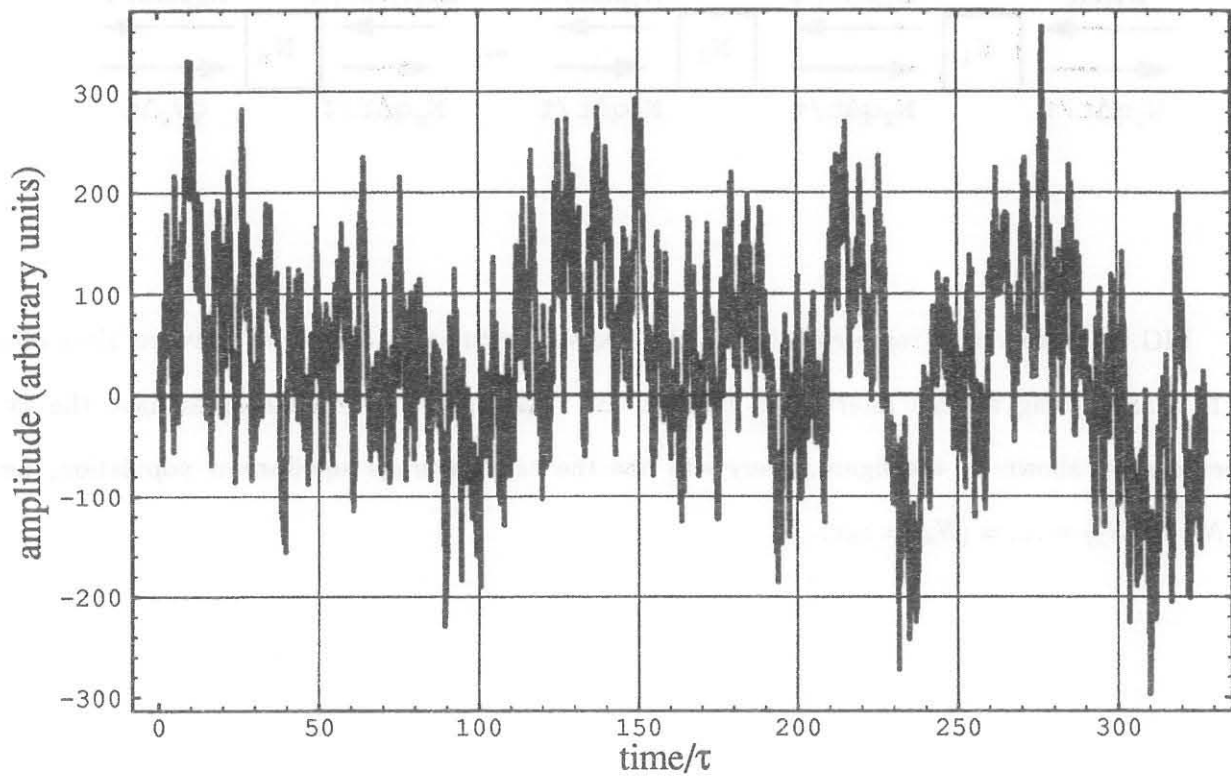
FIG. 10. A small portion (4096 samples) of the simulated signal for a 2D transport channel $(n_x = 20, n_z = 45)$ with a noise source at each end of the channel (the signal is the population fluctuation at the center of the channel. The relaxation time is $\tau = 0.25$ and the simulation step is $\Delta t = 0.02$ (arbitrary time units).
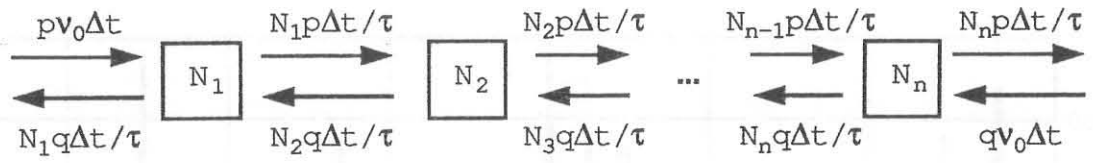
FIG. 11. Schematic representation of the average population exchanges between sites of a 1D chain during a time interval of duration Δt. When the external sources have the average rates shown in the figure, every site has the same average equilibrium population, i.e. $\langle N_1 \rangle = \langle N_2 \rangle = \ldots = \langle N_n \rangle = \nu_0 \tau$.